

# INSERTION DEVICES R&D AT KSRS

I.D. Karpushov, E.Yu. Klimenko, V.A. Mokhnatuk, S.I. Novikov, A.S. Khlebnikov, A.V. Smirnov,  
V.G. Stankevich, A.G. Valentinov, V.A. Bazylev and A.V. Tulupov.  
RRC KI, Moscow 123182, Russian Federation

## Abstract

Current and future plans on wigglers and undulators R&D at the Kurchatov Synchrotron Radiation Source are summarized. Design parameters and performance features of electromagnetic IDs are presented. One of the devices considered can provide suppression of on-axis total power due to a combination of fundamental and third magnetic field harmonics. The key parameters measured as well as the results of 3D magnetostatic and radiation fields computations are discussed.

## 1 INTRODUCTION

There are 9 straight 3m segments available for installation undulators and wigglers at Kurchatov Synchrotron Radiation Source (KSRS). The following beam parameters of KSRS storage ring [1] were used below: e. b. energy  $E=2.5$  GeV, injection energy  $E=0.45$  GeV, beam current  $I=0.1$  A, emittances  $\epsilon_x=104$  nrad,  $\epsilon_y=1.4$  nrad.

The sources to be installed at KSRS have to produce radiation in the wide range 10 eV to 10 keV of photon energies. Two kinds of insertion devices are considered to cover this range: electromagnetic undulator and superconducting wiggler (see Table 1).

Table 1: ID parameters

ID type	EMundulator	SC wiggler
Period $\lambda_w$ , mm	300	130
Maximum strength parameter, $K_w$	7.8	43.7
Number of poles	12	25
Vertical gap $g$ , mm	27	40
Critical photon energy, keV	0.71	9.7

## 2 ELECTROMAGNETIC UNDULATOR WITH REDUCED HEAT LOAD

The main destination of this source is to meet user requirements in the range of 10-250 eV of photon energies, and 10eV is the most important energy for existing VUV users. The structure was optimised to provide reduced heat load for photon energy 10 eV and the ease of fabrication. The design of planar wiggler developed here is based on the concept [2] of on-axis power reduction due to third harmonic of the wiggler magnetic field.

### 2.1 Radiation properties

The optimisation was made for the most critical energy 10 eV in a several steps: the undulator fields was approximated with a few as two harmonics, then the radiation was computed using magnetostatic fields calculated from 2D and 3D computations. We have calculated and plotted below the following value:  $\frac{P_H/F_H}{P_S/F_S}$ , named here as relative power or relative heat

load. Here  $P_S$ ,  $P_H$  are the radiation power for pure sinusoidal wiggler and wiggler containing harmonics for given aperture radius;  $F_S$ ,  $F_H$  are the maximum spectral flux density for pure sinusoidal wiggler and wiggler containing harmonics for given photon energy. This value is useful to demonstrate the effect of the harmonic content on the heat load.

One can see from the Figure 1., that the optimal ratio between harmonics is  $B_3/B_1=0.86$  for the photon energy 10 eV, that gives reduction of relative heat load by 3.65 times.

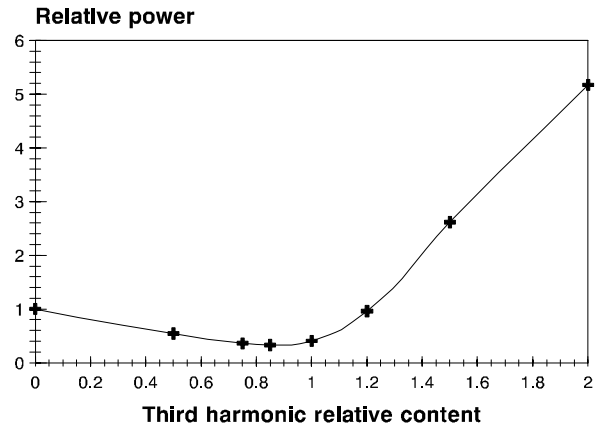


Figure 1. Relative heat load versus  $B_3/B_1$  harmonic amplitude ratio at small aperture and for  $K_w=6.13$ .

For real structure the effect can be influenced by higher order field harmonics. On the Figure 2 the bottom curve corresponds to one of the electromagnetic wiggler designs with  $g=30$  mm gap and magnetic fields calculated with the help of 2D code [3]. The 5<sup>th</sup> harmonic ( $B_5/B_1=0.22$ ) leads to increase of relative heat load (e.g., for small aperture we have 0.52 instead of optimal 0.27).

### 2.2 Undulator design

A number of designs including ones having adjustable harmonic content was considered to provide the optimum

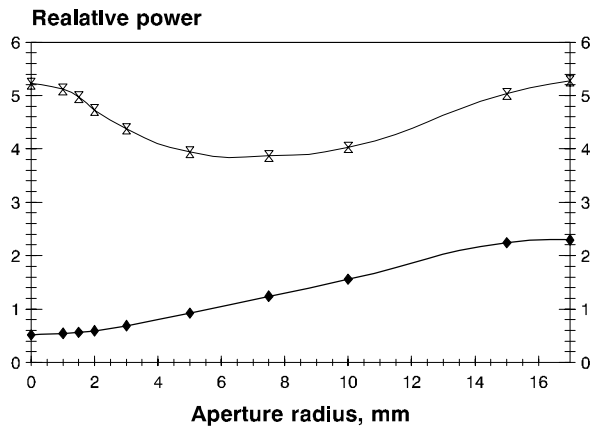


Figure 2. Relative heat load versus aperture radius for different harmonic content:  $B_3/B_1=2$ ,  $B_5=0$  (top curve);  $B_3/B_1=0.85$ ,  $B_5/B_1=0.22$  (down curve). The distance is 10m, spot radius is 4mm for the fundamental line with photon energy 10 eV ( $Kw=6.13$ ).

relationship between the harmonics. The most simple final design has resulted from computations with both 2D [3] and 3D codes [4] (see Figure 3, Figure 4).

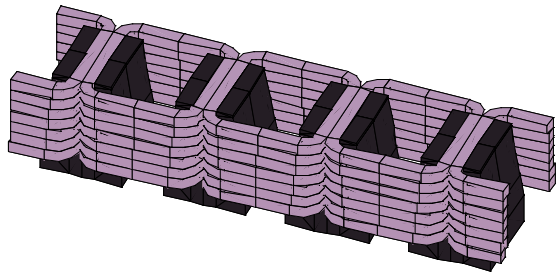


Figure 3. Fragment of EM wiggler (Radia code [4] graphics).

### 3 SC WIGGLER

The SC wiggler is now under designing (see Figure 5). Upper and lower sections of wiggler winding consist of 20 layers of flat racetracks each wound with Nb<sub>3</sub>Sn-bronze conductor (1x4 mm<sup>2</sup> cross section) with thermal of iron sheets (0.8 mm). The design (see Table 2) provides stiffness of the winding and reliable fixing of the SC conductor along it's whole length [5]. An iron insert is placed in a bore of every racetrack. Columns of the inserts form iron poles. A developed method of continuous winding of the racetracks allows to bound a

number of conductor pieces by 14 and to provide total resistance of soldered contacts as low as  $2 \cdot 10^{-8}$  Ohm.

The winding is suspended with stainless steel tubes to a cold platform supported with four titanium alloy supports. Lengths of the tubes and supports are fitted to keep the same position of a wiggler axis before and after cooling. Two thermal shields (80 and 30K) surround the winding. The shields as well as the winding are cooled with helium gas flowing in tubes adhesive bonded to every iron sheet of the winding, to the shields and to the platform. The flows are cooled to operating temperatures in heat exchangers attached to corresponding cold fingers of a three level cryocooler.

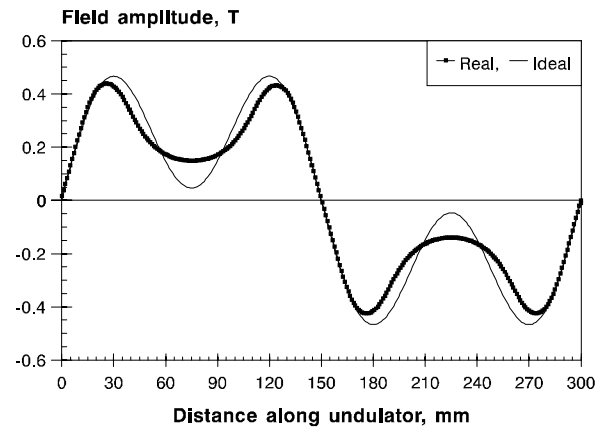


Figure 4. Undulator field shape for real case (measured data and 3D computations:  $B_3/B_1=0.71$ ,  $B_5/B_1=0.15$ ) and for ideal case (two harmonics  $B_3/B_1=0.86$ ).

Table 2: SC wiggler specific parameters

Number of racetracks layers	20x2
Number turns in a racetrack	16
Operating current, A	2000
Operating temperature, K	5.1
Maximum Field at the winding, T	7.2

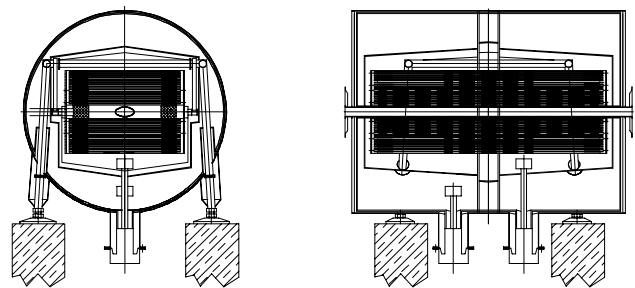


Figure 5. General layout of the SC wiggler.

### 4 EFFECTS OF THE IDs ON THE STORED ELECTRON BEAM

The SC wiggler will be installed in the section of KSRS lattice [6] having zero dispersion in the centre. EM

undulator will be installed in the other section having minimal angular spread .

The tolerances for ID multipole components were determined on the base of canonical perturbation theory. The limiting values for the close orbit horizontal distortions 1mm and tune shift  $\Delta\nu < 5 \cdot 10^{-3}$  were adopted for the estimations of linear and non-linear aberrations as well as resonances induced by ID multipole components. Generated distortions of the beta-functions were limited by 6%. For the EM undulator the 3<sup>rd</sup> and 5<sup>th</sup> harmonics were taken into account [7]. The predefined tolerances for the area  $\pm 10$ mm are summarised in Table 3.

Table 3: ID tolerances

Integrated component	EM undulator, (hor., vert.)	SC wiggler, (hor., vert.)
1 <sup>st</sup> integral, T·m	$<(1.4, 2.4) \cdot 10^{-4}$	$<(2, 6) \cdot 10^{-4}$
2 <sup>nd</sup> integral, T·m <sup>2</sup>	$<(1.6, 1.5) 10^{-4}$	$<(11, 6) \cdot 10^{-4}$
Quadrupole, T	$<(1.6, 1.1) 10^{-2}$	$<(2.5, 4.3) 10^{-2}$
Sextupole, T/m	$<0.51$	$<1.64$
Octupole, T/m <sup>2</sup>	$<120$	$<550$

In addition to integrated components the maximum values of  $\partial^2 B_w / \partial x^2$  were determined in terms of both tune shift analytically and dynamic aperture numerically. The corresponding values are 720 T/m<sup>2</sup> for SC wiggler and 900, 690 T/m<sup>2</sup> for the 1<sup>st</sup> and 3<sup>rd</sup> harmonics correspondingly for the EM undulator.

The influence of SC KRSR wiggler radiation effect on e. b. emittance and energy spread was estimated in terms of Synchrotron Radiation Integrals [8]. The curves based on the existing lattice adjustment and e. b. parameters are plotted on the Figure 6.

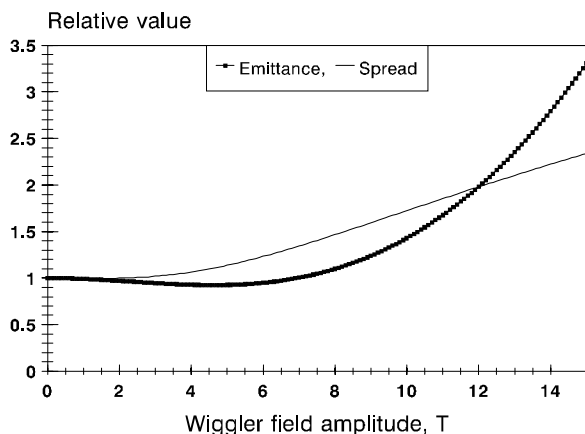


Figure 6. Effect of SC wiggler on relative values of horizontal emittance (thick curve) and energy spread (thin curve).

## ACKNOWLEDGEMENTS

The authors would like to thank Dr. N.V. Smolyakov for the code used for calculation of radiation properties; Dr. P. Elleaume and Dr. O. Chubar for the 3D code Radia

[4] and comprehensive support on the magnetostatic calculations with this code.

## REFERENCES

- [1] Yu. Krylov, V. Stankevich, V. Ushkov, A. Valentinov, Yu. Uupinov, A. Zabelin, A. Filipchenko, V. Korchuganov, U. Ushakov, Status of KRSR, VAL2055, EPAC'98 Conf. Proc.
- [2] A.S. Khlebnikov, N.V. Smolyakov, S.V. Tolmachev and O.V. Chubar. VUV-Wiggler Scheme with Non-Sinusoidal Magnetic Field Profile for High Energy Storage Rings, Proc. of the EPAC 96 Conf., Barseilone, June 1996, p. 2558
- [3] 'POISSON/SUPERFISH Reference Manual', Los Alamos Accelerator Code Group, LANL report LA-UR-87-126 (1987)
- [4] P. Elleaume, O. Chubar, J. Chavanne, Computing 3D Magnetic Field from Insertion Devices, Presented at the PAC97 Conference May 1997, Vancouver; O. Chubar, P. Elleaume, J. Chavanne, A 3D Magnetostatics Computer Code for Insertion devices, to be published in the Proc. of the SRI97 Conf. August 1997, Himeji, Japan.
- [5] P.A.Chernomykh, V.K.Fedorov, E.Yu.Klimenko, V.N.Lunin, S.I.Novikov, A plane Separator for Laboratory studies, *IEEE Trans on Magnetics* 1988, v.24, N2?, p.882-885. E.Yu.Klimenko, S.I.Novikov, V.I.Omelyanenko, S.A.Sergeev, Superconducting Magnet for High Speed Ground Transportation, *Cryogenics*, 1990 v30, N1, p.41-45.
- [6] A. Filipchenko, E. Gornieker, A. Kalinin, V. Korchuganov, G. Kulipanov, G. Kurkin, E. Levichev, Yu. Matveev, V. Sajiev, V. Ushakov, A. Kadnikov, Yu. Krylov, D. Odintsov, S. Pesterev, V. Stankevich, V. Ushkov, A. Valentinov, Yu. Yupinov, A. Zabelin. Siberia-2: Work in Progress. Proc. of the EPAC 96 Conf., Barseilone, June 1996, p. 608
- [7] A.V. Smirnov. On the analysis of periodic magnetostatic systems. *Nucl. Instrum. and Meth.* NIM A349 (1994)295.
- [8] R. Helm et al., *IEEE Trans. Nucl. Sci.*, NS-20, 900 (1973).